Characterization of *Helicobacter pylori* γ-Glutamyltranspeptidase Reveals the Molecular Basis for Substrate Specificity and a Critical Role for the Tyrosine 433-Containing Loop in Catalysis[†,‡]

Amy L. Morrow, Kristin Williams, Aaron Sand, Gina Boanca, and Joseph J. Barycki*

Department of Biochemistry, University of Nebraska, 1901 Vine Street, Lincoln, Nebraska 68588-0664

Received August 9, 2007; Revised Manuscript Received September 6, 2007

ABSTRACT: *Helicobacter pylori* γ-glutamyltranspeptidase (HpGT) is a member of the N-terminal nucleophile hydrolase superfamily. It is translated as an inactive 60 kDa polypeptide precursor that undergoes intramolecular autocatalytic cleavage to generate a fully active heterodimer composed of a 40 kDa and a 20 kDa subunit. The resultant N-terminus, Thr 380, has been shown to be the catalytic nucleophile in both autoprocessing and enzymatic reactions. Once processed, HpGT catalyzes the hydrolysis of the γ-glutamyl bond in glutathione and its conjugates. To facilitate the determination of physiologically relevant substrates for the enzyme, crystal structures of HpGT in complex with glutamate (1.6 Å, R_{factor} = 16.7%, R_{free} = 19.0%) and an inactive HpGT mutant, T380A, in complex with *S*-(nitrobenzyl)glutathione (1.55 Å, R_{factor} = 18.7%, R_{free} = 21.8%) have been determined. Residues that comprise the γ-glutamyl binding site are primarily located in the 20 kDa subunit and make numerous hydrogen bonds with the α-amino and α-carboxylate groups of the substrate. In contrast, a single hydrogen bond occurs between the T380A mutant and the remainder of the ligand. Lack of specific coordination beyond the γ-glutamyl moiety may account for the substrate binding permissiveness of the enzyme. Structural analysis was combined with site-directed mutagenesis of residues involved in maintaining the conformation of a loop region that covers the γ-glutamyl binding site. Results provide evidence that access to this buried site may occur through conformational changes in the Tyr 433-containing loop, as disruption of the intricate hydrogen-bond network responsible for optimal placement of Tyr 433 significantly diminishes catalytic activity.

Infection by the human pathogen *Helicobacter pylori* places an individual at risk for developing gastritis, peptic ulcer disease, and gastric adenocarcinoma (*1*, *2*). The primary site of infection is the mucus layer of the gastric epithelium, where specific adaptations have allowed the bacterium to exploit its microenvironment and evade immune response. *H. pylori* γ-glutamyltranspeptidase (HpGT)[1] has been identified as a virulence factor (*3*, *4*), but its precise role in colonization and persistence remains elusive. HpGT has been shown to induce apoptosis in gastric epithelial cells (*5*, *6*), upregulate COX-2 and epidermal growth factor-related peptides in human gastric mucosal cells (*7*), and inhibit T-cell proliferation (*8*). Each of these physiological responses depends on the enzymatic activity of the protein, but the mechanisms by which the enzyme's products trigger these effects have not been determined, in part because its range of substrates and products are not fully characterized.

Recent studies have shown that HpGT enables *H. pylori* to degrade extracellular glutamine and glutathione, generating glutamate that can be transported into the organism for use in the tricarboxylic acid cycle and glutamine synthesis (*9*). Thus, HpGT-dependent depletion of host extracellular glutathione and glutamine pools, possibly coupled with the resulting production of ammonia from glutamine hydrolysis, may contribute to gastric epithelial cell damage. In patients infected with *H. pylori*, the concentration of glutathione in the gastric mucosa is significantly lowered compared to *H. pylori*-negative patients suggesting that the bacteria deplete this critical antioxidant (*10*). To understand the impact of bacterial metabolism on the host epithelium, more detailed characterization of the HpGT metabolites is needed.

HpGT and other γ-glutamyltranspeptidases (γGT) are members of the N-terminal nucleophile (Ntn) hydrolase enzyme family (*11*). Ntn hydrolases are synthesized as inactive precursors that must undergo intramolecular autocatalytic cleavage to gain enzymatic activity (*12*, *13*). The resulting N-terminal residue, typically a serine, threonine, or cysteine, is the nucleophile in both the processing and hydrolase reactions. HpGT is translated as an inactive 60 kDa polypeptide that spontaneously autoprocesses into a 40

[†] This publication was made possible by NIH Grants P20 RR-17675 from the National Center for Research Resources and 1R01 GM077289 (J.J.B.). Use of the Advanced Photon Source was supported by the U.S. Department of Energy, Basic Energy Sciences, Office of Science, under Contract W-31-109-Eng-38. Use of BioCARS Sector 14 was supported by the National Institutes of Health, National Center for Research Resources, under Grant RR07707.

* Address correspondence to this author: phone (402) 472-9307; fax (402) 472-7842; e-mail jbarycki2@unl.edu.

[‡] Coordinates and structure factors have been deposited in the Protein Data Bank under accession codes 2QM6 and 2QMC.

[1] Abbreviations: HpGT, *Helicobacter pylori* γ-glutamyltranspeptidase; γGT, γ-glutamyltranspeptidase; GNA, L-glutamic acid γ-(4-nitroanilide)

10.1021/bi701599e CCC: $37.00
Published on Web 10/26/2007

kDa/20kDa heterodimer (*4*, *14*). In solution, the protein exists primarily as a heterotetramer composed of two heterodimers, and the N-terminal nucleophile is a conserved threonine residue, Thr 380 (*14*). γGT are generally thought to be involved in the metabolism of glutathione. The γ-glutamyl group is cleaved from the glutathione tripeptide via an acyl-enzyme intermediate and is transferred to water in a hydrolysis reaction or to an amino acid or small peptide in a transpeptidation (*14*−*19*). Interestingly, HpGT exhibits limited transpeptidase activity as compared to eukaryotic homologues and is capable of using either glutamine or glutathione as a substrate, suggesting that the enzyme is a general γ-glutamyl hydrolase (*4*, *14*).

Previously, we described the crystal structure of HpGT and demonstrated that autoprocessing results in the formation of a threonine−threonine catalytic dyad that is required for efficient catalysis (*20*). Despite visualization of architectural details and putative catalytic residues in the apoenzyme structure, the molecular basis for substrate binding and specificity was not entirely unambiguous. Therefore, in this paper, these studies have been extended to identify the substrate binding site of the enzyme and to examine ligand entry into the active site. Structures of HpGT with bound glutamate and an inactive HpGT mutant complexed with *S*-(nitrobenzyl)glutathione have been determined. Examination of the refined models indicates that the γ-glutamyl moiety is the primary binding determinant and that an adjacent solvent-exposed cavity allows for significant promiscuity with respect to the remainder of the substrate. Mutational analysis supports a model in which an active-site loop regulates substrate access and is required for optimal enzymatic activity.

MATERIALS AND METHODS

Overexpression, Purification, and Crystallization of HpGT. Wild-type HpGT and the mature T380A mutant were expressed in *Escherichia coli* and purified from the soluble lysate by affinity chromatography on a nickel-chelating column (Novagen) as described previously (*4*, *14*). Additional point mutations were introduced at residues D421, N431, Y433, and Q506 using the QuikChange site-directed mutagenesis kit (Stratagene) following the manufacturer's protocol, and all constructs were verified by sequencing (Genomics Core at the University of Nebraska−Lincoln). Protein crystals were grown at 18 °C by the sitting drop method out of a solution of 200 mM HEPES, pH 7.5, within the precipitant range of 20−30% poly(ethylene glycol) 2000 monomethyl ether at a final protein concentration of 5 mg/mL (*20*). Prior to data collection, crystals were transferred to artificial mother liquor containing 30% poly(ethylene glycol) 2000 monomethyl ether, as well as the ligand of interest, and flash-frozen in liquid nitrogen.

Data Collection, Model Building, and Refinement. Diffraction data ($\lambda = 0.9$ Å; 100 K) were collected on Beamline 14-BM-C of BioCARS at Argonne National Laboratory's Advanced Photon Source and analyzed with the HKL2000 software package (*21*). HpGT structures were determined by molecular replacement using MOLREP (*22*), with wild-type HpGT apoenzyme (PDB ID 1NQO; *20*) as the search molecule. Iterative rounds of model building and refinement were performed using the programs (Crystallographic Object)-Oriented Toolkit (COOT; *23*) and REFMAC5 (*24*), respectively. An R_{free} test set (10%) was maintained to monitor refinement. As the model neared completion, TLSMD (*25*) was used to identify optimal multigroup TLS models for use in REFMAC (*26*). Water molecules obeying proper hydrogen-bonding constraints with electron densities greater than 1.0σ on a $2F_o - F_c$ map and 3.0σ on an $F_o - F_c$ map were also included in the final structure. Model geometry was monitored with MOLPROBITY (*27*) and figures were produced with Chimera (*28*).

Kinetic Characterizations of HpGT. Autoprocessing of the HpGT precursor (60 kDa) to its mature form (20 kDa and 40 kDa subunits) results in enzymatic activity (*14*). To quantify the processing rate, mutant or wild-type HpGT was incubated in 20 mM Tris buffer, pH 8.0 at 37 °C. At the indicated time, an aliquot was removed and enzymatic activity was measured by monitoring the hydrolysis of the substrate analogue, L-glutamic acid γ-(4-nitroanilide) (GNA; Sigma) on a Cary 50 spectrophotometer (0.1 M Tris buffer, pH 8.0; 1 mM GNA; 25 °C). Data were plotted as a function of time and fit to a first-order monoexponential curve with Prism (Graph Pad Software). Complete maturation was verified by SDS−PAGE. Representative data from three or more determinations are presented with experimental errors determined from individual fits of the kinetic data. Apparent kinetic constants were determined by assaying enzymatic activity at various concentrations of GNA, ranging from 1 to 1000 μM (*17*, *29*), and the data were fit by use of the Michaelis−Menten equation.

RESULTS AND DISCUSSION

Identification of the γ-Glutamyl Binding Site of HpGT. Our initial objective was to capture either the Michaelis complex of HpGT with various substrates or the γ-glutamyl acyl enzyme intermediate. Apoenzyme HpGT crystals were transferred to artificial mother liquor containing cryoprotectant and various substrates and rapidly frozen in liquid nitrogen. When the chromogenic GNA substrate was used, the protein crystals immediately turned yellow, indicative of intact HpGT catalytic activity within the crystal lattice (data not shown). X-ray diffraction data to ≥1.6 Å were collected on HpGT crystals incubated with GNA (data not shown), oxidized glutathione (data not shown), and reduced glutathione (Table 1). In each case, an examination of the electron density at the enzyme active site was consistent with glutamate bound to the enzyme active site. Therefore, complete refinement was carried out only with HpGT crystals that had been soaked with reduced glutathione (Table 1). The resulting HpGT−glutamate complex was refined to 1.6 Å resolution with an overall $R_{factor} = 16.7\%$ ($R_{free} = 19.0\%$). A complete heterotetramer (two large subunits, two small subunits) was contained within the asymmetric unit. The final model contains 10 residues with alternate conformations and has >97% of all residues in the favored region of the Ramachandran plot (*27*). Interestingly, Asn 400 in each of the 20 kDa subunits of the heterotetramer had unusual backbone conformations ($\phi \sim 84°$, $\psi \sim -106°$), which may implicate this residue in maintenance of the active-site architecture.

The overall structure of a single heterodimer illustrates the relative position of the substrate binding domain with

Table 1: Data Collection and Refinement Statistics for the *H. pylori* γ-Glutamyltranspeptidase Structures

	HpGT + glutamate	T380A + *S*-(nitrobenzyl)glutathione
Data Collection Statistics		
space group	$P2_1$	$P2_1$
cell dimensions, Å	54.98, 104.76, 91.91, $b = 91.85$	57.14, 106.67, 87.19, $b = 104.96$
resolution, Å	32.9−1.60 (1.66−1.60)	33.4−1.55 (1.61−1.55)
no. of unique reflections	136 302	135 161
avg redundancy	6.5 (4.8)	6.6 (5.0)
$\langle I/\sigma I \rangle$	21.9 (2.7)	21.3 (2.6)
completeness, %	99.4 (99.3)	93.2 (89.0)
R_{sym},[a] %	8.8 (47.4)	8.4 (53.8)
Refinement Statistics		
no. of atoms	8885	8684
protein atoms	8128	8066
solvent atoms	737	588
ligand atoms	20	30
R_{factor}, %	16.7 (18.7)	18.7 (22.0)
R_{free}, %	19.0 (23.8)	21.8 (26.5)
overall *B* factor, Å^2	15.4	21.2
protein *B* factor, Å^2	14.3	20.7
solvent *B* factor, Å^2	27.7	26.0
rmsd from ideal values		
bond lengths, Å	0.010	0.011
bond angles, deg	1.23	1.35
estimated coordinate error (Luzzati), Å	0.09	0.10

[a] $R_{sym} = \Sigma|I - \langle I \rangle|/\Sigma I$.

bound glutamate (Figure 1A). Glutamate is depicted at the enzyme active site proximal to the N-terminal nucleophile, Thr 380. Well-defined electron density is observed for glutamate, which is one of the products of glutathione hydrolysis (Figure 1B). The γ-glutamyl binding site is composed of residues almost entirely in the 20 kDa subunit (Figure 1C, green), with only Arg 103 of the 40 kDa subunit contributing to glutamate binding (Figure 1C, purple). The α-amino group of glutamate forms hydrogen bonds with the side chains of Asn 400, Glu 419, and Asp 422, whereas the α-carboxylate is coordinated directly and indirectly (via a bridging water molecule) by Arg 103, Ser 451, and Ser 452. This hydrogen-bond network in HpGT is likely the basis for substrate binding. Support for this conclusion derives from the previously reported mutational analysis of human γGT by Meister and co-workers (*30*−*32*). Substitution of Asp 423 (equivalent to Asp 422 in HpGT) increased the K_m for GNA by >2000-fold for the hydrolysis reaction (*32*). Replacement of Arg 107 (Arg 103 in HpGT) also significantly impacted substrate binding (*31*). In human γGT, substitution of either Ser 451 or Ser 452 with an alanine residue resulted in a 27- or 15-fold reduction in V_{max}, respectively, but only a modest 4-fold increase in K_m in both cases (*30*). Given their central role in coordinating the α-carboxylate of the γ-glutamyl group (Figure 1C), it is somewhat surprising that removal of either Ser 451 or Ser 452 does not dramatically alter the K_m for GNA. However, one possibility is that in the S451A and S452A mutants, a water molecule functionally compensates by occupying the site normally filled with the side-chain hydroxyl groups of these highly conserved serine residues. A recent report indicates that a S451A/S452A HpGT double mutant lacks enzymatic activity (*8*), but detailed kinetic characterizations were not presented. A nearly identical active-site configuration is observed in *E. coli* γGT (*33*). The only difference is the isosteric, conservative substitution of glutamate, Glu 419 in HpGT, by a glutamine residue, Gln 430 in *E. coli* γGT. Collectively, these results suggest that the γ-glutamyl binding site is likely to be structurally conserved in all γ-glutamyltranspeptidases.

Delineation of the Cysteinylglycine Binding Pocket. To identify the remainder of the substrate binding site, crystals of an inactive but processed HpGT mutant were prepared. A bicistronic construct designed to express the 40 kDa and the 20 kDa subunits separately but concurrently was used to generate a mature enzyme devoid of enzymatic activity as described previously (T380A; *14*). This strategy was necessary because it is unlikely that the substrate binding site is adequately formed in the unprocessed T380A mutant (*34*). Mature T380A was crystallized under similar conditions as the wild-type enzyme. Various ligands, including reduced glutathione, oxidized glutathione, and *S*-(nitrobenzyl)glutathione, were soaked into mature T380A crystals during cryoprotection. X-ray diffraction data were collected for each complex and the resultant electron density maps were examined. For oxidized (1.8 Å) and reduced (1.6 Å) glutathione complexes, the ligand exhibited considerable mobility beyond the γ-glutamyl group, preventing the inclusion of the remainder of the molecule in the crystallographic model (data not shown).

The T380A−*S*-(nitrobenzyl)glutathione complex provided the greatest insight into the location of the cysteinylglycine binding pocket (Table 1). The refined structure (1.55 Å, R_{factor} = 18.7%, R_{free} = 21.8%) contains γ-glutamylcysteine modeled at the active site of the protein (Figure 2). Whereas the γ-glutamyl portion of the ligand is rigidly held in place by numerous hydrogen bonds, a single hydrogen bond is observed between the cysteinyl amide group and the backbone carbonyl of Asn 400. Relatively weak density was observed for the cysteinyl moiety of *S*-(nitrobenzyl)glutathione, consistent with flexibility in the bound ligand. In addition, several small negative and positive peaks observed in the difference map beyond γ-glutamylcysteine suggest the presence of alternate conformations. A comparable qualitative fit to the observed electron density was obtained by exchanging the thiol and carbonyl functionalities of the cysteinyl

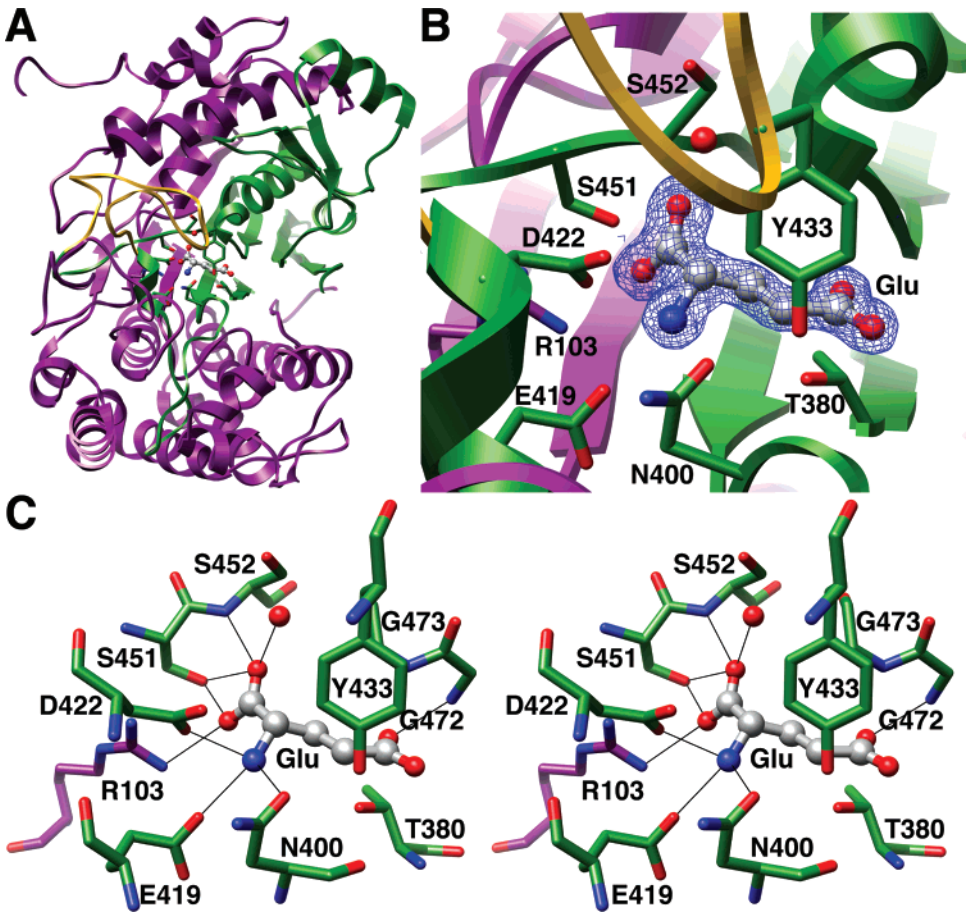

FIGURE 1: Structural details of the γ-glutamyl binding site of HpGT. **(**A**)** Ribbon representation of the overall HpGT topology. The 40 kDa subunit is colored in purple, the 20 kDa subunit in green, and a mobile active-site loop containing Tyr 433 in yellow. Pertinent active-site residues are shown in stick representation and the bound glutamate in ball and stick representation. Oxygen atoms are shown in red and nitrogen atoms in blue. **(**B**)** Electron density corresponding to the bound glutamate superimposed on a magnification of the active site. The relevant $2F_o - F_c$ electron density is contoured at 1.5σ and colored in blue. The majority of the ligand is buried within the core of HpGT. Residues discussed in the text are labeled. **(**C**)** Stereodiagram of the HpGT−glutamate hydrogen-bond network. Potential hydrogen bonds between HpGT and glutamate are illustrated as black lines. The bound glutamate is held rigidly in place by at least nine hydrogen bonds, primarily involving the amino acid backbone.

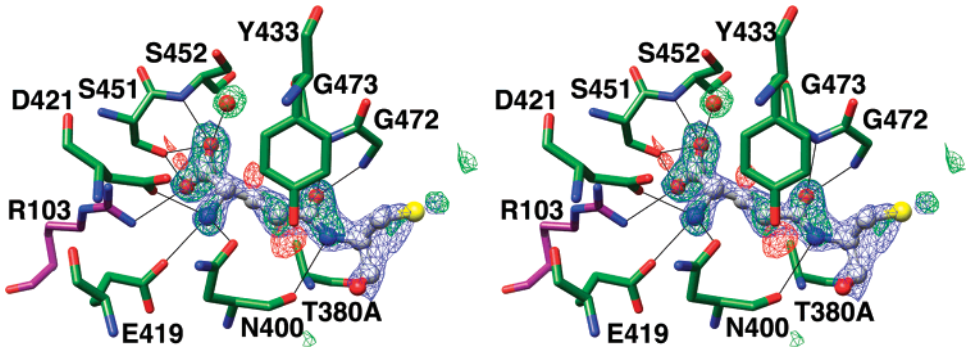

FIGURE 2: Binding of *S*-(nitrobenzyl)glutathione to an inactive HpGT mutant. The structure of a processed but inactive HpGT mutant, T380A, was determined in complex with *S*-(nitrobenzyl)glutathione. Atoms are colored and depicted as in Figure 1, with the sulfur atom of the ligand colored in yellow. Also shown are the calculated electron density maps after the initial round of refinement, prior to inclusion of the ligand in the model. The relevant $2F_o - F_c$ electron density is contoured at 1.00σ and illustrated in blue. Positive and negative peaks in the difference map, contoured at 3.5σ, are shown in green and red, respectively. The electron density rapidly deteriorates beyond the γ-glutamylcysteinyl moiety, suggesting considerable conformational flexibility.

group (data not shown). However, this possibility was excluded because in this orientation, there would not be a cavity to accommodate the nitrobenzyl ring of the ligand. Though increased mobility of the cysteinylglycine group could be the result of the T380A substitution, only minor perturbations in the T380A structure relative to that of the wild-type enzyme were observed (Figure 3A; discussed below). Furthermore, an examination of the adjacent pocket does not reveal an obvious candidate for the glycine binding site. Although there is a solvent-exposed cleft that could accommodate glycine, functionally conserved groups that would coordinate the terminal carboxylate of glutathione are not readily apparent. Collectively, these data indicate that HpGT primarily recognizes the γ-glutamyl group of its

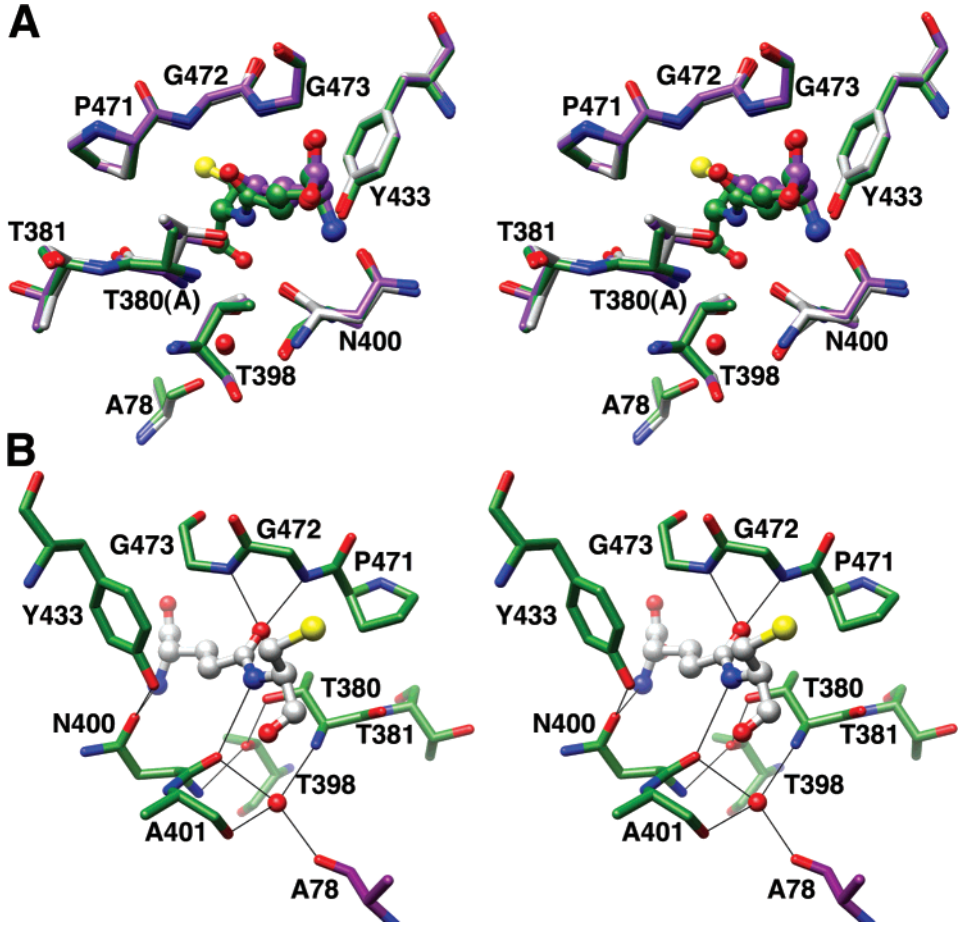

FIGURE 3: Generation of a Michaelis complex model. **(**A**)** Comparison of HpGT active-site structures. In the stereodiagram, the refined structures of the apoenzyme (gray), the HpGT−glutamate complex (purple), and the T380A−S-(nitrobenzyl)glutathione complex (green) have been superimposed. Nearly identical placements of atoms are observed with the exception of the slight displacement of Ala 380 in the T380A mutant structure. **(**B**)** Model of wild-type HpGT in complex with a γ-glutamylcysteinyl group. The T380A−*S*-(nitrobenzyl)glutathione complex structure was modified, replacing Ala 380 with a threonine residue positioned similarly to the wild-type enzyme. The resulting model, colored as in Figure 1, suggests that as the side-chain hydroxyl of Thr 380 attacks the γ-glutamyl peptide bond during catalysis, its α-amino group would be positioned optimally to protonate the leaving group.

substrates and has a poorly defined cysteinylglycine binding site.

The lack of a defined cysteinylglycine binding site is consistent with observed kinetic differences between HpGT and human γGT (*14*, *32*). Activity of the human enzyme is stimulated nearly 200-fold by the presence of glycylglycine, the standard acceptor group used to measure transpeptidase activity. In contrast, HpGT shows a modest increase (∼2-fold) under similar conditions. As the cysteinylglycine and the acceptor binding sites are thought to be overlapping (*35*), these observations suggest that HpGT may be a general γ-glutamyl hydrolase with broad substrate specificity instead of an enzyme tailored for glutathione degradation with potentially adventitious γ-glutamyl transpeptidation activity. Recent studies that compared the reactivity of human and *E. coli* γGT with a series of γ-phosphonodiester analogues of glutamate demonstrated that human γGT exhibits a clear specificity for analogues with a carboxylate group that would be spatially equivalent to the carboxylate of glutathione, whereas *E. coli* γGT shows no such requirement (*36*). However, modeling studies of the human enzyme do not suggest obvious candidate functional groups that would coordinate the cysteinylglycine portion of the substrate (*20*, *37*), and additional structural studies of the mammalian γGT are needed.

Comparison of HpGT Structures and Modeling of the Michaelis Complex. The T380A−S-(nitrobenzyl)glutathione structure was superimposed on those of the wild-type apoenzyme and glutamate-bound HpGT (Figure 3A). Overall, the rms deviation between pairs of heterodimers is ≤0.3 Å, suggesting that gross conformation changes do not occur during the catalytic cycle. A detailed examination reveals that active-site residue placements are strictly conserved. However, in the T380A−*S*-(nitrobenzyl)glutathione complex, the substituted alanine residue is displaced slightly relative to the corresponding threonine residue in the wild-type protein. To generate a model of the Michaelis complex, the catalytic threonine residue, Thr 380, was incorporated back into the T380A complex structure, maintaining a position comparable to that observed in the two wild-type structures (Figure 3B).

In the modeled Michaelis complex, Thr 380 would be positioned optimally for nucleophilic attack of the γ-glutamyl peptide bond. As described previously, the nucleophilicity of the threonine hydroxyl group is likely increased through stabilizing interactions with its own α-amino group and the side-chain hydroxyl of a second conserved threonine residue, Thr 398 (*20*, *33*). The subsequent formation of the tetrahedral intermediate would be stabilized by the backbone amides of Gly 472 and Gly 473. Proceeding through the transition state,

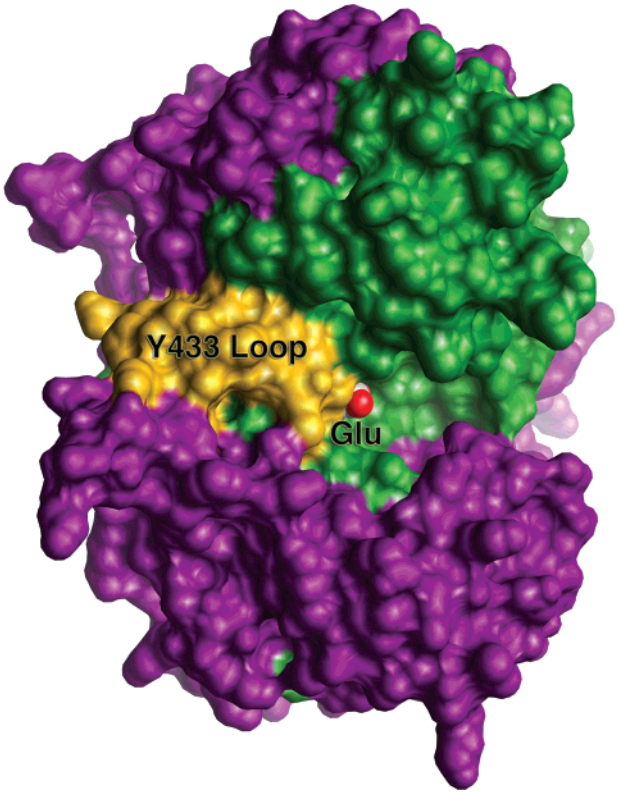

FIGURE 4: The γ-glutamyl binding site is buried in HpGT. The solvent-accessible surface of HpGT was calculated and colored as in Figure 1. Only the γ-carboxylate of the bound glutamate is solvent-accessible. A potentially mobile loop (colored in yellow) containing a functionally conserved residue, Tyr 433, may adopt alternate conformations to allow substrate entry into the active site. A solvent-exposed cavity that could accommodate the cysteinylglycine of the glutathione substrate is adjacent to the γ-glutamyl binding site.

the α-amino group of Thr 380 would be in close proximity to the cysteinyl nitrogen of the substrate and may protonate the cysteinylglycine leaving group. As modeled in Figure 3B, the interatomic distance between these groups is 3.6 Å. However, formation of the tetrahedral intermediate would likely shorten this distance by ~1 Å. Recent kinetic characterizations of rat γGT used a discontinuous HPLC-based assay with glutathione and glutathione derivatives as substrates (*37*). Results of this study support a mechanism in which a rate-limiting nucleophilic attack by the active-site threonine is rapidly followed by the protonation and exit of the amine leaving group.

Contributions of the Tyr 433-Containing Loop to Catalysis. Inspection of the final HpGT−glutamate structure indicates that the γ-glutamyl portion of the substrate is buried deep in the core of the protein (Figure 4), suggesting local conformational changes must precede ligand binding. One potential binding scenario would have the loop containing Tyr 433 (colored yellow in Figure 4) gating the active site; movement of this loop would allow substrate binding. To test this hypothesis, the hydrogen-bond network responsible for proper placement of the Tyr 433-containing loop (Figure 5) was probed by mutational analysis of selected residues (designated by asterisks).

Tyr 433 is oriented over the γ-carboxylate in the HpGT-glutamate bound structure and may occlude solvent from the site of reaction. Its side-chain hydroxyl can form a hydrogen bond with the side chain of Asn 400, a highly conserved residue with unusual ϕ and ψ angles that appears to be important in both substrate binding and catalysis. Mutagenesis of Asn 400 yielded insoluble protein, suggesting that substitutions at Asn 400 significantly destabilize the enzyme. However, two soluble point mutations of Tyr 433 were purified and characterized. Removal of the Tyr 433 hydroxyl group (Y433F) led to a >7-fold increase in the K_m for GNA, whereas the complete removal of the phenolic side chain produced only a modest 2-fold increase in K_m (Table 2). The implication of these results is that the Asn 400−Tyr 433 hydrogen bond orients the Tyr 433 side chain, thereby preventing it from occluding the substrate binding site in the unbound state. This interaction is not required for efficient catalysis, as the Y433F mutant has comparable catalytic activity to the wild-type enzyme. Interestingly, bacterial γGT tend to maintain a tyrosine residue at this position whereas in eukaryotic γGT, a phenylalanine residue is often substituted. This variation may contribute to the observed differences in enzymatic properties (*20*, *33*). The importance of maintaining either a phenylalanine or a tyrosine residue at this position was investigated by use of the Y433A mutant. Although substrate binding was not impacted significantly, the enzyme retained only 4% activity relative to wild-type HpGT (Table 2). These collective results support a critical but noncatalytic role for Tyr 433. A probable explanation is that Tyr 433 shields the active site from solvent during catalysis and/or stabilizes the local active-site architecture.

To further examine the contributions of the Tyr 433-containing loop to catalysis, additional mutations were made in residues involved in its positioning. The side-chain carboxylate of Asp 421 forms a hydrogen bond with the backbone amide of Leu 432 and with a water molecule that positions the side chains of Asp 422 and Asn 400 for optimal substrate binding. Substitution of Asp 421 with an asparagine (D421N) or a serine (D421S) had only minor impacts on the K_m for GNA (Table 2). However, the D421S mutant had 36-fold reduced catalytic activity, comparable to that observed in the Y433A mutant. The D421N mutant was only 1.6-fold less active, suggesting that the ability of Asp 421 to participate in the extensive hydrogen-bond network, rather than its electrostatic character, is needed for efficient catalysis. Furthermore, the relative inactivity of D421S confirms that bifurcated hydrogen-bonding potential is critical. A comparable substitution in human γGT, D422A, resulted in a considerably different outcome (*32*). This mutation produced approximately a 10-fold increase in K_m with virtually no effect on catalysis. In HpGT, Asp 421 forms a hydrogen bond with the backbone amide of Leu 432 (Figure 5), thus stabilizing the position of the active-site loop. In human γGT, this leucine is replaced with a glutamate residue, Glu 432, which could form compensatory hydrogen bonds to stabilize the Tyr 433-containing loop. As indicated above, subtle perturbations in this mobile active-site loop may contribute to observed catalytic differences.

The side chains of Asn 431 and Gln 506 can form hydrogen bonds with the backbone amide and carbonyl groups of Tyr 433, respectively. As with the Asp 421 mutants, substitution of Asn 431 with a serine (N431S) or Gln 506 with an alanine (Q506A) had modest effects on the K_m for GNA (Table 2). However, both mutants were catalytically impaired at a level that was comparable to the

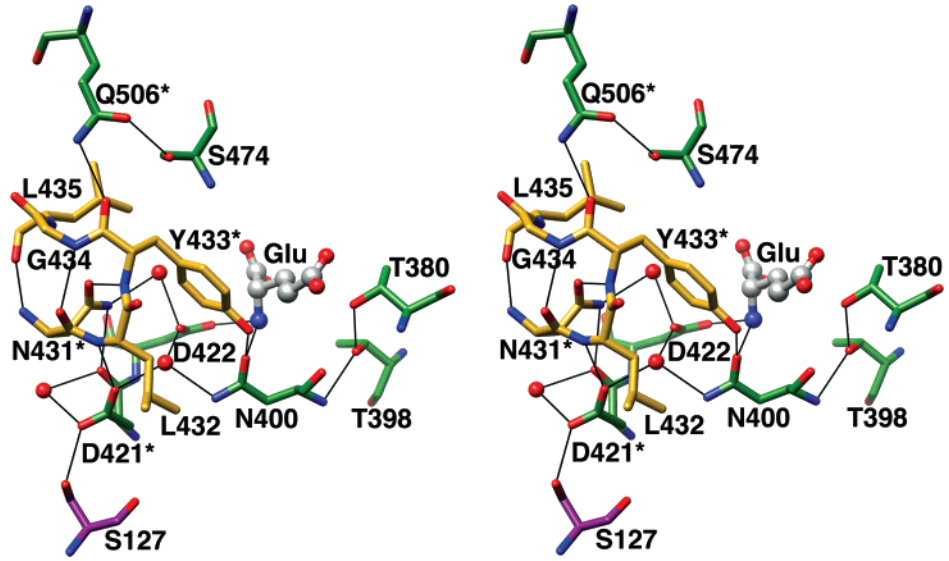

FIGURE 5: Positioning of the Tyr 433-containing loop. The stereodiagram illustrates the intricate hydrogen-bond network involved in stabilizing the Tyr 433-containing loop. Carbon atoms from the 40 kDa subunit are shown in purple, the 20 kDa subunit in green, and the Tyr 433-containing loop in yellow. Functionally conserved residues selected for site-directed mutagenesis studies are designated with asterisks. Tyr 433 appears to shield the active site from solvent and thus contribute to the enzymatic efficiency of the enzyme. Disruption of this hydrogen-bond network reduces enzymatic activity significantly.

Table 2: Apparent Kinetic Constants for Wild-type and Mutant HpGT

	hydrolysis		processing
enzyme	K_m GNA (μM)	V_{max} (μmol min^{-1} mg^{-1})	$t_{1/2}$ (min)
HpGT	38.3 ± 3.8	5.04 ± 0.13	49.3 ± 5.3
Y433A	82.2 ± 5.4	0.20 ± 0.01	84.6 ± 0.6
Y433F	284 ± 8.3	4.33 ± 0.06	63.6 ± 6.8
Q506A	16.7 ± 1.9	0.18 ± 0.01	93.6 ± 7.7
N431S	53.6 ± 6.6	0.12 ± 0.01	55.2 ± 6.2
D421N	59.3 ± 3.4	3.24 ± 0.05	73.8 ± 7.3
D421S	67.7 ± 5.8	0.14 ± 0.01	130 ± 12.2

effect of Y433A substitution. Thus, each of the residues predicted to stabilize the Tyr 433-containing loop contributes to catalysis significantly and to a similar extent. The minor structural perturbations that result from the alteration of these highly conserved residues likely increase the overall mobility of the Tyr 433-containing loop. These substitutions also impair the autocatalytic processing of the enzyme to a limited extent (Table 2), suggesting this mobile loop may perform a peripheral function during maturation.

Recently, the structure of a mutant *E. coli* γGT incapable of maturation was described (*34*). In the unprocessed enzyme structure, the linker region connecting the 40 kDa and 20 kDa subunits spanned the substrate binding site and resulted in the displacement of the analogous tyrosine containing loop in *E. coli* γGT. In addition, the authors reported a metal-bound *E. coli* γGT structure with disorder in this loop region as well. Preliminary structural studies of an inactive precursor HpGT (3.5 Å; G.B. and J.J.B., unpublished observation) also suggest the Tyr 433-containing loop must move to accommodate the linker region that joins the large and small subunits prior to autoprocessing. Our structural and mutational studies support a mechanism in which the Tyr 433 loop opens to allow substrate binding. Interestingly, in both the *E. coli* and *H. pylori* apoenzyme structures, the tyrosine-containing loop adopts a "closed" conformation that is stabilized, at least in the crystal lattice, by an extensive hydrogen-bond network. In the HpGT apoenzyme structure, a tightly bound water molecule is observed in the active site at a position equivalent to that of the α-amino group of the γ-glutamyl substrate. This ordered water forms hydrogen bonds with the side chains of Asn 400, Glu 419, and Asp 422 and may help stabilize the observed "closed" conformation. It is unclear what triggers this necessary local domain movement and additional studies to examine the dynamics of this region are ongoing.

ACKNOWLEDGMENT

We thank the BioCARS staff for assistance in X-ray data collection, Dr. Mark Wilson (University of Nebraska) for helpful discussions, and Dr. Melanie Simpson (University of Nebraska) for her thoughtful insights and review of the manuscript.

REFERENCES

1. Sharma, P., and Vakil, N. (2003) Review article: *Helicobacter pylori* and reflux disease, *Aliment. Pharmacol. Ther. 17*, 297−305.
2. Bjorkholm, B., Falk, P., Engstrand, L., and Nyren, O. (2003) *Helicobacter pylori*: resurrection of the cancer link, *J. Intern. Med. 253*, 102−119.
3. McGovern, K. J., Blanchard, T. G., Gutierrez, J. A., Czinn, S. J., Krakowka, S., and Youngman, P. (2001) γ-Glutamyltransferase is a *Helicobacter pylori* virulence factor but is not essential for colonization, *Infect. Immun. 69*, 4168−4173.
4. Chevalier, C., Thiberge, J. M., Ferrero, R. L., and Labigne, A. (1999) Essential role of *Helicobacter pylori* γ-glutamyltranspeptidase for the colonization of the gastric mucosa of mice, *Mol. Microbiol. 31*, 1359−1372.
5. Shibayama, K., Kamachi, K., Nagata, N., Yagi, T., Nada, T., Doi, Y., Shibata, N., Yokoyama, K., Yamane, K., Kato, H., Iinuma, Y., and Arakawa, Y. (2003) A novel apoptosis-inducing protein from *Helicobacter pylori*, *Mol. Microbiol. 47*, 443−451.
6. Kim, K. M., Lee, S. G., Park, M. G., Song, J. Y., Kang, H. L., Lee, W. K., Cho, M. J., Rhee, K. H., Youn, H. S., and Baik, S. C. (2007) γ-glutamyltranspeptidase of *Helicobacter pylori* induces mitochondria-mediated apoptosis in AGS cells, *Biochem. Biophys. Res. Commun. 355*, 562−567.
7. Busiello, I., Acquaviva, R., Di Popolo, A., Blanchard, T. G., Ricci, V., Romano, M., and Zarrilli, R. (2004) *Helicobacter pylori*

γ-glutamyltranspeptidase upregulates COX-2 and EGF-related peptide expression in human gastric cells, *Cell. Microbiol. 6*, 255−267.
8. Schmees, C., Prinz, C., Treptau, T., Rad, R., Hengst, L., Voland, P., Bauer, S., Brenner, L., Schmid, R. M., and Gerhard, M. (2007) Inhibition of T-cell proliferation by *Helicobacter pylori* γ-glutamyl transpeptidase, *Gastroenterology 132*, 1820−1833.
9. Shibayama, K., Wachino, J., Arakawa, Y., Saidijam, M., Rutherford, N. G., and Henderson, P. J. (2007) Metabolism of glutamine and glutathione via γ-glutamyltranspeptidase and glutamate transport in *Helicobacter pylori*: possible significance in the pathophysiology of the organism, *Mol. Microbiol. 64*, 396−406.
10. Jung, H. K., Lee, K. E., Chu, S. H., and Yi, S. Y. (2001) Reactive oxygen species activity, mucosal lipoperoxidation and glutathione in *Helicobacter pylori*-infected gastric mucosa, *J. Gastroenterol. Hepatol. 16*, 1336−1340.
11. Suzuki, H., and Kumagai, H. (2002) Autocatalytic processing of γ-glutamyltranspeptidase, *J. Biol. Chem. 277*, 43536−43543.
12. Oinonen, C., and Rouvinen, J. (2000) Structural comparison of Ntn-hydrolases, *Protein Sci. 9*, 2329−2337.
13. Brannigan, J. A., Dodson, G., Duggleby, H. J., Moody, P. C., Smith, J. L., Tomchick, D. R., and Murzin, A. G. (1995) A protein catalytic framework with an N-terminal nucleophile is capable of self-activation, *Nature 378*, 416−419.
14. Boanca, G., Sand, A., and Barycki, J. J. (2006) Uncoupling the enzymatic and autoprocessing activities of *Helicobacter pylori* γ-glutamyltranspeptidase, *J. Biol. Chem. 281*, 19029−19037.
15. Tate, S. S., and Meister, A. (1981) γ-Glutamyl transpeptidase: catalytic, structural and functional aspects, *Mol. Cell. Biochem. 39*, 357−368.
16. Taniguchi, N., and Ikeda, Y. (1998) γ-Glutamyl transpeptidase: catalytic mechanism and gene expression, *Adv. Enzymol. Relat. Areas Mol. Biol. 72*, 239−278.
17. Keillor, J. W., Castonguay, R., and Lherbet, C. (2005) γ-glutamyl transpeptidase substrate specificity and catalytic mechanism, *Methods Enzymol. 401*, 449−467.
18. Ikeda, Y., and Taniguchi, N. (2005) Gene expression of γ-glutamyltranspeptidase, *Methods Enzymol. 401*, 408−425.
19. Allison, R. D. (1985) γ-Glutamyl transpeptidase: kinetics and mechanism, *Methods Enzymol. 113*, 419−437.
20. Boanca, G., Sand, A., Okada, T., Suzuki, H., Kumagai, H., Fukuyama, K., and Barycki, J. J. (2007) Autoprocessing of *Helicobacter pylori* γ-glutamyltranspeptidase leads to the formation of a threonine-threonine catalytic dyad, *J. Biol. Chem. 282*, 534−541.
21. Otwinowski, Z., and Minor, W. (1997) Processing of X-ray Diffraction Data Collected in Oscillation Mode, *Methods Enzymol. 276*, 307−326.
22. Vagin, A., and Teplyakov, A. (1997) MOLREP: an Automated Program for Molecular Replacement, *J. Appl. Crystallogr. 30*, 1022−1025.
23. Emsley, P., and Cowtan, K. (2004) Coot: model-building tools for molecular graphics, *Acta Crystallogr. D: Biol. Crystallogr. 60*, 2126−2132.
24. Murshudov, G. N., Vagin, A. A., and Dodson, E. J. (1997) Refinement of macromolecular structures by the maximum-likelihood method, *Acta Crystallogr. D: Biol. Crystallogr. 53*, 240−255.
25. Painter, J., and Merritt, E. A. (2006) TLSMD web server for the generation of multi-group TLS models, *J. Appl. Crystallogr. 39*, 109−111.
26. Winn, M. D., Isupov, M. N., and Murshudov, G. N. (2001) Use of TLS parameters to model anisotropic displacements in macromolecular refinement, *Acta Crystallogr, D: Biol. Crystallogr. 57*, 122−133.
27. Lovell, S. C., Davis, I. W., Arendall, W. B., 3rd, de Bakker, P. I., Word, J. M., Prisant, M. G., Richardson, J. S., and Richardson, D. C. (2003) Structure validation by Calpha geometry: phi,psi and Cbeta deviation, *Proteins: Struct., Funct., Genet. 50*, 437−450.
28. Pettersen, E. F., Goddard, T. D., Huang, C. C., Couch, G. S., Greenblatt, D. M., Meng, E. C., and Ferrin, T. E. (2004) UCSF Chimera−a visualization system for exploratory research and analysis, *J. Comput. Chem. 25*, 1605−1612.
29. Tate, S. S., and Meister, A. (1985) γ-Glutamyl transpeptidase from kidney, *Methods Enzymol. 113*, 400−419.
30. Ikeda, Y., Fujii, J., Anderson, M. E., Taniguchi, N., and Meister, A. (1995) Involvement of Ser-451 and Ser-452 in the catalysis of human γ-glutamyl transpeptidase, *J. Biol. Chem. 270*, 22223−22228.
31. Ikeda, Y., Fujii, J., and Taniguchi, N. (1993) Significance of Arg-107 and Glu-108 in the catalytic mechanism of human γ-glutamyl transpeptidase. Identification by site-directed mutagenesis, *J. Biol. Chem. 268*, 3980−3985.
32. Ikeda, Y., Fujii, J., Taniguchi, N., and Meister, A. (1995) Human γ-glutamyl transpeptidase mutants involving conserved aspartate residues and the unique cysteine residue of the light subunit, *J. Biol. Chem. 270*, 12471−12475.
33. Okada, T., Suzuki, H., Wada, K., Kumagai, H., and Fukuyama, K. (2006) Crystal structures of γ-glutamyltranspeptidase from *Escherichia coli*, a key enzyme in glutathione metabolism, and its reaction intermediate, *Proc. Natl. Acad. Sci. U.S.A. 103*, 6471−6476.
34. Okada, T., Suzuki, H., Wada, K., Kumagai, H., and Fukuyama, K. (2007) Crystal structure of the γ-glutamyltranspeptidase precursor protein from *Escherichia coli*. Structural changes upon autocatalytic processing and implications for the maturation mechanism, *J. Biol. Chem. 282*, 2433−2439.
35. Thompson, G. A., and Meister, A. (1977) Interrelationships between the binding sites for amino acids, dipeptides, and γ-glutamyl donors in γ-glutamyl transpeptidase, *J. Biol. Chem. 252*, 6792−6798.
36. Han, L., Hiratake, J., Kamiyama, A., and Sakata, K. (2007) Design, synthesis, and evaluation of γ-phosphono diester analogues of glutamate as highly potent inhibitors and active site probes of γ-glutamyl transpeptidase, *Biochemistry 46*, 1432−1447.
37. Morin, M., Rivard, C., and Keillor, J. W. (2006) γ-Glutamyl transpeptidase acylation with peptidic substrates: free energy relationships measured by an HPLC kinetic assay, *Org. Biomol. Chem. 4*, 3790−3801.

BI701599E